

Mop Moiré Patterns Using MopNet

Bin He¹ Ce Wang¹ Boxin Shi^{1,2} Ling-Yu Duan^{1,2}

National Engineering Lab for Video Technology, Peking University, Beijing, China¹
The Peng Cheng Laboratory, Shenzhen, China²

Fcs.hebi n, wce, shi boxi n, l i ngyuG@pku. edu. cn

Abstract

Moiré pattern is a common image quality degradation caused by frequency aliasing between monitors and cameras when taking screen-shot photos. The complex frequency distribution, imbalanced magnitude in colour channels, and diverse appearance attributes of moiré pattern make its removal a challenging problem. In this paper, we propose a Moiré pattern Removal Neural Network (MopNet) to solve this problem. All core components of MopNet are specially designed for unique properties of moiré patterns, including the multi-scale feature aggregation to address complex frequency, the channel-wise target edge predictor to exploit imbalanced magnitude among colour channels, and the attribute-aware classifiers to characterize the diverse appearance for better modelling Moiré patterns. Quantitative and qualitative comparison experiments have validated the state-of-the-art performance of MopNet.

1. Introduction

With the widespread use of smart phones and the booming of social media, nowadays the digital images occupy an indispensable part in our everyday life for capturing and sharing memorable moments or useful information. However, when people take a shot of the content in front of the monitors, there are often occasions when the images are contaminated by undesired moiré artifacts as shown in the upper row of Figure 1. Moiré pattern is a kind of artifact caused by frequency aliasing, particularly interference between overlapping patterns like the grids of display elements and camera sensors. The appearance of moiré patterns can be rather diverse and complex, shaped in spatially varying stripes, curves or ripples. Moiré patterns also superimpose colour variations onto images, drastically degrading the visual quality of images.

Removing the undesired patterns from a moiré image is an image restoration problem, but it is not trivial to ana-

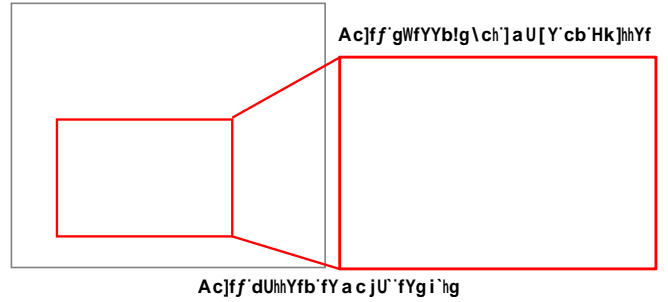


Figure 1: Undesired Moiré patterns are often observed on an image captured in front of the monitor (upper row). MopNet is proposed to more cleanly remove such patterns than state-of-the-art methods (e.g., DMCNN [20]).

lytically write down the moiré image formation model due to its complex properties: 1) the moiré pattern signal spans a broad frequency spectrum mixed with natural images, 2) the imbalanced colour distribution of the colour filter array (CFA) makes moiré patterns show different intensities in RGB colour channels respectively, and 3) the appearance of moiré patterns, especially the shape, not only varies from image to image, but also changes locally within the same image. These complex properties pose unique challenges to moiré pattern removal problem.

To remove moiré patterns, an anti-aliasing low-pass filter [17] can be added to the camera, however the optical filter causes the loss of high-frequency information and results in over-smoothed images. Post-processing algorithms for removing moiré artifacts is a more often used solution. Existing methods [15, 22] mostly resort to signal processing theory and explore low-rank and sparsity constraint, but they cannot deal with complex moiré patterns other than

Ling-Yu Duan is the corresponding author.

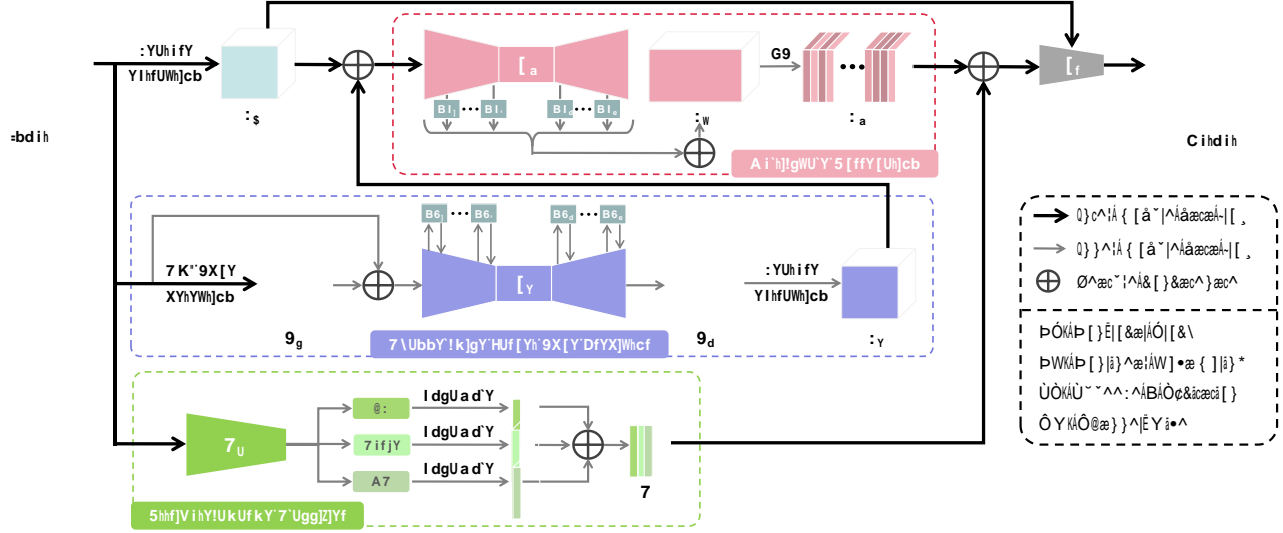


Figure 2: The framework of our proposed method MopNet, consisting of three major functional modules: the multi-scale feature aggregation to exploit the complex distribution of moiré pattern in a broad frequency range, the channel-wise target edge predictor to estimate edge map of moiré-free image, and the attribute-aware classifier to classify the moiré pattern with multiple appearance attribute labels.

those in highly textured images. Recently, a deep neural network based method [20] has been proposed to implicitly model the moiré pattern through learning from a large-scale dataset; though better restored images than non-learning approaches are produced, the performance significantly drops for moiré images taken in the wild (with different capture settings from the training data), as shown in bottom left of Figure 1, partially due to the lack of specific constraints addressing unique properties of moiré patterns.

In this paper, to better exploit the properties of moiré patterns and conquer the corresponding challenges, we propose a **Moiré pattern Removal Neural Network** named **MopNet** to “mop” moiré patterns from images, as shown in Figure 2. We observe three key properties of moiré patterns by investigating their frequency distribution, edge intensities, and appearance categories, and integrate these properties to design learning modules for MopNet. Thanks to the property oriented designs, MopNet provides a cleaner removal for moiré contaminated images as shown in bottom right of Figure 1. Our contributions can be summarized as follows:

- We propose a property oriented learning framework for moiré pattern removal. With discovered properties of moiré patterns from multiple aspects including frequency distribution, edge information and appearance attributes, our framework contributes to the comprehensive modelling of moiré patterns.
- We propose specific learning schemes to resolve these useful properties. Particularly, we come up with the multi-scale feature aggregation, channel-wise edge predictor, and attribute-aware classifier, to deal with issues of the complex frequency distribution, imbal-

anced edge intensities among colour channels, as well as appearance diversity of moiré patterns, respectively.

- We have achieved cleaner moiré removal in the benchmark datasets including those challenging low-frequency moiré patterns. Our approach may better preserve the structure of target images, which outperforms state-of-the-art methods in terms of numerical metrics and subjective visual quality. Moreover, we make additional annotation of attributes over benchmark datasets, which is useful to improve the performance via the property oriented learning framework.

2. Related Work

Moiré pattern removal. Moiré pattern is a common degradation to digital images due to frequency aliasing of sampling in image formation and greatly degrades the image, however the research of moiré pattern removal has been mainly limited to physics and optical field, with analysis of display devices on hardware level [18]. A few computational methods have also been proposed on demoiréing in the past decade. Conventional signal processing based techniques [15, 22] have been adopted like low-rank constrained and sparse matrix decomposition in frequency domain. Though those methods achieve good results in moiré pattern removal for highly-textured images, they often fail to handle screen-shot images. Layer decomposition method [23] is also proposed to remove screen-shot moiré pattern, but the process is time-consuming with limited success.

Recently, with the revolution in low-level vision led

Figure 3: Frequency spectrum of images of Gaussian noise, rain streak, moiré pattern, and a natural scene.

by deep learning, convolutional neural networks based demoiréing method has also emerged. Kim *et al.* [7] proposed an adversarial and content-aware learning framework to implement de-screening only for the net-shaped moiré patterns in scanned images. Sun *et al.* [20] proposed a multi-scale CNN to learn the mapping to moiré-free images, with a benchmark dataset captured on LCD screens of various models. Liu *et al.* [13] presented a similar work with GAN framework and a synthesized dataset simulating the camera imaging process. These works do not explicitly explore specific properties of moiré artifacts, and sometimes over smooth the images due to the lack of exploitation on subtle edge structures.

Learning based image restoration. Image restoration has been a classical research field with many branches for various image degradations. The problem of moiré pattern removal is also one of them, with some common characteristics, yet poses many unique challenges as well. In the recent deep learning era, numerous image restoration works show impressive results benefited from the learning scheme. To handle a wide range of different noises, multiple designs such as multi-layer perceptron [2] and residual learning based convolutional neural networks [28, 10] are adopted. Recently many works focus on the removal of rain streaks in images, utilizing the advantage of generative adversarial network [26] and specifically exploiting the density information of rain streak patterns [25] to recover clean images. Besides, other distortions such as haze [24] and blur [16] are also investigated for image restoration, with specific physics models introduced [24]. Also, general degradation oriented universal learning framework has been investigated, with prior of degradation kernel [28] or exploitation of self-similarity through non-local operation [14]. Yet for the common contamination of moiré patterns in images, less research has been made, especially those taking advantage of deep learning. Existing image restoration methods might not be effective for handling moiré patterns due to the diversity in shape and complexity in colour and frequency.

3. Methodology

In this section, we will describe the details of the proposed MopNet, the methodology for networks designs, and the details for training. As illustrated in Figure 2, MopNet consists of three major functional modules which will be introduced in details in Sections 3.1, 3.2, and 3.3. The overall pipeline and the training details are provided in Section 3.4 and Section 3.5 respectively.

3.1. Multi-scale feature aggregation

Moiré patterns are complex in terms of the distribution in frequency domain. As can be observed in the Fourier spectrum in Figure 3, the moiré pattern within a single image tends to cover a broad range of frequency bands. In addition, we find that compared with the spectrum of Gaussian noise, the frequency of moiré pattern is more concentrated at the low frequency band, making moiré patterns indistinguishable from ordinary moiré-free images. Besides, the spectrum of moiré patterns shows variation in more diverse directions than those of rain streak images, with multiple response peaks in frequency domain. Therefore exploring complex properties of moiré patterns in frequency domain is necessary for efficient removing. Accordingly, we propose to aggregate multi-scale features in networks to fully consider the frequency characteristic of moiré patterns, as shown in the first row of Figure 2.

We propose to extract the multi-scale features from the bottleneck blocks similar to the ones in [5], with receptive field of different sizes. Then the features are fused by a concatenation and squeeze-and-excitation (SE) block [4]. SE block computes normalized weights for each channel, and feature maps are re-weighted by multiplying the weights learned by SE block. The aggregated feature produced from this module can be presented mathematically as follows:

$$F_m = SE(Cat[NU_1(F_1), NU_2(F_2), \dots, NU_n(F_n)]), \quad (1)$$

where SE stands for the operations of the SE block, *Cat* indicates concatenation, F_i denotes feature maps of different frequency bands obtained from multi-scale extractor g_m , and NU_i is a non-linear upsampling used to convert feature maps to the same spatial size.

Note that our multi-scale feature aggregation scheme differs from the parallel branches design with inputs of different resolutions in [20]. We utilize the SE block to concatenate the convolutional features instead of the linear superposition of the results from different scales. This implementation helps to extensively exploit the pattern features within a broader range of frequency, and selectively emphasize the features from the scales corresponding to dominant frequency bands with SE block.

Figure 4: Edge maps for a grayscale image¹ and RGB channels. The region highlighted by the yellow box shows the different magnitudes of moiré effects in each edge map.

3.2. Channel-wise target edge predictor

The majority of moiré patterns are shaped in curves and stripes with significant edge magnitude. To address such an edge sensitive task, the edge cue is a common choice, which is proved to be effective in various layer separation problems [11, 12]. Particularly, we find that for a typical Bayer color filter array (CFA) [1], the sampling frequency of R, B channels is half that of G channel, which makes R, B channels tend to be more aliased according to the Nyquist theorem. Such imbalance in colour channels is more obvious on moiré patterns than natural images, which is reflected as stronger edge intensities in R, B channels as shown in Figure 4. We, therefore, assume moiré pattern edges are more likely to be separated when edge magnitude in colour channels are more imbalanced. So we propose to separate the edge maps of target contents and those of moiré patterns through a channel-wise target edge predictor, whose inputs are the contaminated images and their channel-wise edge maps (as shown in the second row of Figure 2).

We apply a network to predict the channel-wise edge map E_p for the moiré-free target image I_t , with a given source image I_s . Considering the imbalance of edge on RGB channels, we augment the source image I_s with its separate edge maps of each colour channel E_{sr}, E_{sg}, E_{sb} convoluted with Sobel kernels, instead of the grayscale edge map. Our edge predictor maps such an augmented input to the target edge map E_p :

$$E_p = \text{Cat}(E_{pr}, E_{pg}, E_{pb}) = g_e(I_s, E_{sr}, E_{sg}, E_{sb}), \quad (2)$$

where g_e denotes the proposed channel-wise edge predictor, and E_{pr}, E_{pg}, E_{pb} stand for predicted edge maps for R, G, B channels. Furthermore, non-local blocks [21] are introduced to assist the predictor in capturing semantic edges with weaker gradient. For each position in a feature map, the non-local block computes correlation weights between

¹The grayscale image is converted from an RGB input by $R = 0.299 + G = 0.587 + B = 0.114$.

Figure 5: Different types of moiré patterns. L: Low frequency, H: High frequency; S: Straight, C: Curve; MC: Multiple Colours, SC: Single Colour.



Figure 6: The distribution of different labels in our training set. We can find that the attribute distributions in each class are approximately equal.

features at that position and the rest, then obtain the response as a weighted sum of the features at all positions. The correlation matrix for a point on a weak edge captures long-distance dependencies, which assists the weak edge to obtain a stronger response by strengthening features at strong edges in weighted summation.

The acquisition of target edge map E^t is essential for the restoration because it helps to guide the reconstruction of the target image I^t while preserving its subtle structures from potential over-smoothing. The channel-wise consideration guides the target edge predictor to better distinguish the edges of moiré patterns from the mixed edges.

3.3. Attributes-aware moiré pattern classifier

The moiré patterns show great diversity in pattern appearance, as shown in Figure 5, which also makes the modelling of moiré patterns from learning and removing various patterns using a single type of network challenging. However we have observed that the diverse patterns show certain obvious attributes that can be categorized, such as different frequencies, shapes, and colours. Therefore we assume extra explicit descriptions of the patterns will guide the learning process, and propose a multi-label classifier c_a to better depict the diversity of moiré patterns by characterizing three appearance attributes including the dominant frequency, colour, and shape of the pattern (as shown in the third row in Figure 2).

We indicate the moiré images by three attribute labels

through multi-label classification, the examples of classified images are illustrated in Figure 5. The attribute labels for the dominant frequency, colour, and shape are binary for easy implementation, and due to the generally balanced data distribution observed on each attribute as shown in Figure 6. By concatenating the three up-sampled label maps, we obtain the pattern attribute information of the input image as:

$$C = \text{Cat}[u(C_0), u(C_1), u(C_2)], \quad (3)$$

where C_0 , C_1 , and C_2 denote the predicted scalars for dominant frequency, shape, and colour; u stands for up-sampling operation which generates a label map filled with corresponding scalar. Then this prediction of pattern attribute is fed into the inference of the target output to provide auxiliary guidance on the pattern appearance.

The frequency label helps to specially deal with the low frequency moiré patterns whose energy is mixed with the image content to avoid over-smoothing the target image when incorrectly treated as high frequency patterns. The colour label emphasizes moiré patterns consisting of more than one colour, which are more complicated for removal by mingling with the original colour of the target image than single colour ones. The shape label draws attention to curved moiré patterns which have more complex curvatures than straight stripes. Hence, these three categorized descriptions of pattern attributes would benefit learning of diverse patterns, which are expected to improve the capability of generalization to patterns unseen in training data.

3.4. Overall pipeline and objective function

As shown in Figure 2, MopNet takes a single image with moiré artifacts as input, then passes it through the three modules to extract the corresponding property features. The features of estimated target edge map F_e are concatenated to the features of input image F_0 . And the features are further aggregated through our multi-scale feature aggregation module to obtain F_m , after which the predicted labels C are also aggregated for the final inference. The moiré-free output is reconstructed by feeding the features of original input F_0 , along with the aforementioned aggregated features into the refinement block g_r . The process can be described as the following formulation:

$$I_o = g_r(\text{Cat}[F_m, C], F_0), \quad (4)$$

where I_o denotes the output of the proposed network, g_r is the non-linear refinement which consists of SE block and cascaded convolution layers.

The classifier is trained with binary cross entropy loss for each attribute. And considering that the CNN feature based perceptual loss helps improve the visual quality of estimated image [26] and enhance semantic edge information [9], we combine weighted pixel-wise Euclidean loss

and the feature-based loss as our objective for training the network. It can be summarized as following:

$$L = L_{E,e} + L_{E,o} + L_F, \quad (5)$$

where $L_{E,e}$ and $L_{E,o}$ represent the per-pixel Euclidean loss function to reconstruct target edge map and ground truth image respectively, λ controls the weight of the loss derived from edge map prediction. And L_F is the feature based loss for the moiré-free image, defined as:

$$L_F = \frac{1}{CWH} \| (I_o) - (I_t) \|_2^2, \quad (6)$$

where ϕ represents a non-linear CNN transformation to extract high-level feature map, and C , W , and H denote the channel number, width and height of the feature map.

3.5. Training details and data preparation

We implement MopNet² using PyTorch framework on a PC with a Intel i7-7700 3.60GHz CPU and NVIDIA 1080 Ti GPU. And we apply a two-stage training strategy. To guarantee a stable initialization of the training procedure, we first train the edge prediction network and classifier independently for 50 and 20 epochs respectively until converge. Then we fix the classifier network and train the entire network end-to-end for 150 epochs. During training for both stages, a 256×256 input is randomly cropped from the input image with the scale 286×286 . We use Adam [8] as optimization algorithm with a mini-batch size of 2. The learning rate is initially set to 0.0002 and is linearly decreased with training proceeding. We use a weight decay of 0.0001 and a momentum of 0.9. We set $\lambda = 0.1$ when fine-tuning the entire network, and compute the feature loss from the layer relu1_2 extracted from the VGG-16 model.

The training and testing dataset we adopt is the benchmark dataset proposed by [20], which consists of 135,000 screen-shot images with moiré artifacts. The dataset is collected from the ImageNet dataset [3], with the original image as the ground truth for moiré-free image, and the moiré images are captured under various imaging conditions.

Besides, to train the desired classifiers for pattern attributes, we randomly sample a subset with 12000 pairs of images, and supplement the subset with multiple pattern attribute labels, including frequency, colour and pattern shape. Then we train MopNet on this supplemented subset, and pre-trained VGG-16 networks are fine-tuned with such attribute labels as the classifiers.

4. Experiments

In this section, we first quantitatively compare the performance of our proposed method against the state-of-the-art learning based moiré pattern removal method DM-CNN [20], traditional signal processing based method [23]

²Detailed network architecture can be found in the supplementary.

Figure 7: Visual quality comparison among MopNet, DMCNN [20], Yang *et al.* [23], and Descreen plugin for Photoshop.

Table 1: Quantitative results evaluated in terms of average PSNR (dB) and SSIM.

	Input	DnCNN	VDSR	U-Net	DMCNN	Ours
PSNR	20.30	24.54	24.68	26.49	26.77	27.75
SSIM	0.738	0.834	0.837	0.864	0.871	0.895

and the related Sattva Descreen plugin³ in image processing software Adobe Photoshop. We further demonstrate whether the moiré artifacts can be effectively handled by other image restoration methods such as DnCNN [27], VDSR [6], and U-Net [19]. To further evaluate the capability of improving image quality visually, we also make a qualitative comparison among those methods. At last, we conduct ablation study for different functional modules for verifying the effectiveness of our proposed network designs.

4.1. Quantitative evaluation

We adopt the widely-used metric for image quality evaluation PSNR and SSIM, and demonstrate the quantitative comparison in Table 1⁴. As exhibited in Table 1, the PSNR and SSIM of the inputs are at a low level, due to the contamination of moiré patterns. We can also observe that the general denoising method DnCNN [27] and super-resolution method [6] have obtained limited image quality improvement compared to moiré-specific methods. That is mainly because they are not designed specifically for the problem of moiré pattern removal, and the flat network structure they adopt cannot effectively handle moiré artifacts with

complex frequency distribution. The state-of-the-art DMCNN [20] delivers better performance, however the multi-resolution scheme it proposed cannot sufficiently exploit the properties of moiré patterns including edges and appearance attributes. Thus its performance on PSNR and SSIM is not evidently better than the U-Net [19] which involves feature links for decoder on different resolutions. As shown in Table 1, MopNet surpasses all other methods, outperforming the existing state-of-the-art method by 0.98dB gain in PSNR. MopNet also provides results that are visually similar to the moiré-free images with a SSIM value of 0.895.

4.2. Qualitative evaluation

The examples of qualitative comparison are shown in Figure 7⁵, where we can observe that the input images are severely moiré-contaminated, with obvious colour deviation and patterns shaped in curves or stripes superimposed on the ground truth clean image. We show a visual quality comparison with Descreen plugin for Photoshop, non-learning based [23] and learning based [20] moiré pattern removal methods. Specifically, the first to the third row in Figure 7 show cases of moiré patterns with different dominant frequency bands, corresponding to low frequency, mixed frequency, and high frequency pattern, respectively. The descreen plugin shows limited effectiveness, because it tends to blur the image, however still leaves the coloured moiré patterns visible. Yang *et al.* [23] cannot effectively deal with the low frequency patterns, as shown in the first and fourth row in Figure 7. DMCNN [20] achieves much better removal results for moiré artifacts. However its capability to erase the low frequency moiré pattern is restricted,

³<http://www.descreen.net/eng/soft/descreen/descreen.htm>

⁴We do not provide the quantitative results for the descreen plugin and yang *et al.* [23] due to that the former requests excessive manual operation of tuning parameters and the latter costs prohibitively long running time (about half an hour per image) for benchmarking, respectively.

⁵More results can be found in the supplementary, based on which we conduct a perceptual study.

Figure 8: Visual quality comparison of different variants of our method. B: Basemodel, M: Multi-scale feature aggregation, C: classifier, E: Edge predictor. The yellow boxes mark regions contain slight differences need a close check.

Table 2: Quantitative results of variants of MopNet.

	PSNR	SSIM
Baseline model	25.377	0.862
Baseline + Multi-scale (MS)	26.617	0.882
Baseline + MS + Classification	27.076	0.884
Baseline + MS + Edge	27.440	0.890
Full model	27.753	0.895

Figure 9: Edge prediction results with different inputs and network architecture. (a) Input image, (b) channel-wise edge map with non-local block, (c) gray image edge map + non-local block, (d) channel-wise edge without non-local block, and (e) ground truth. Please zoom-in for details.

which may leave unexpected coloured spots or stripes on the output image, as shown in the first row of Figure 7.

In contrast, our proposed method more effectively eliminates the low frequency patterns, benefiting from our improved multi-scale feature aggregation scheme. In addition, from the highlighted region of images in the third row of Figure 7, we can find that the edges on the wall existing in reference image are over-smoothed in the procedure of DMCNN [20] restoration, on the contrary our method more faithfully preserves such subtle structure of the original image with the help of the prediction of target edges.

4.3. Ablation study

To validate the effectiveness of our specific network designs for moiré pattern removal, we conduct ablation experiments on models without such functional modules or learning schemes for comparison. The numerical quality of restored moiré-free images is shown in Table 2. Based on the controlled experiments, it can be seen that the proposed designs all contribute to the performance gain of the PSNR and SSIM of restored images.

The visual comparison for different variants of our model is shown in Figure 8⁶. From the first row in Figure 8, we can find there remain wide light-coloured stripes in the result of the baseline method in the region marked by the yellow box. In contrast, the model with multi-scale feature aggregation scheme can more completely remove such low frequency moiré stripes. And in the second row of Figure 8, we can tell that models without edge predictor destroy the structure of the thin wires marked by the yellow box because of over-smoothing. In contrast, the exploitation of edge information offers constraints to better maintain the subtle structures in original moiré-free image. And from the last row it can be observed that after adding the appearance classification, the complex curves on the background marked by the yellow box is cleanly removed.

We also have investigated the effectiveness of the schemes in edge prediction. Examples of target edge maps predicted with and without the separate edge maps for RGB channels and non-local blocks are illustrated in Figure 9. By observing region marked by yellow boxes, We can find that when fed with single grayscale edge map of mixture

⁶More results can be found in supplementary.

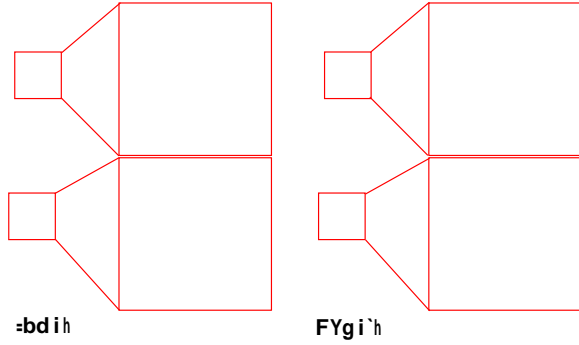


Figure 10: Moiré pattern removal results for texture images using MopNet.

image as input, the predicted target edge map cannot thoroughly get rid of the edges of moiré patterns in background, while the channel-wise edge maps on separate RGB channel can lead to more accurate target edge prediction without obvious moiré residual. Also we can infer from the regions marked by red boxes that the non-local blocks also contribute to better target edge prediction.

5. Discussions

Moiré patterns in texture images. Apart from the aliasing between monitors and cameras, in the real world there also exists moiré artifacts caused by the fine repetitive textures on materials like cloth or tiles. To test the capability of generalization of MopNet on images that are not included in our training data, we test our model on textured images searched from the Internet. As shown in Figure 10, though there exist no direct moiré-free reference images, it can be observed that our restored results effectively get rid of the coloured moiré curves while maintaining its subtle textures of cloth or bricks. Note that our MopNet is trained with screen-shot moiré images and have never seen such moiré images caused by sophisticated texture, it can generalize well on textured data in the wild.

High resolution moiré images. Due to the limitation of the resolution of partial data in training dataset and GPU memory, we train our model on 256×256 images, which is the same size as the input in DMCNN [20]. This problem of limitation in input size can be partially solved through downsampling the high resolution inputs, and increasing the resolution of output with pre-trained super-resolution networks [9]. As shown in Figure 11, the high resolution output obtained in such a way highly resembles the high resolution ground truth visually. Still, a direct end-to-end solution for high resolution moiré images will be included in our future work.

6. Conclusion

We proposed MopNet, consisting of a multi-scale aggregated, edge-guided, and pattern attribute-aware network to

Figure 11: A case of removal result for high resolution moiré image. LR, SR, and HR stand for low resolution, super resolution, and high resolution respectively.

Figure 12: Examples of images containing complex and irregular texture, compared with DMCNN [20]. The regions highlighted by yellow boxes show the mixture of moiré and complex texture.

“mop” moiré patterns from images. It exploits and specially deals with the properties of moiré patterns including complex frequency distribution, imbalanced intensities of edges among RGB channels and varying appearance attributes. Quantitative and qualitative experiments demonstrated that our method has outperformed existing state-of-the-art methods. In the future, we will attempt to further investigate the formation mechanism of moiré patterns for cleaner “mopping”, and we believe such a post-processing solution for this problem will benefit the vast users of smartphones for capturing and sharing moiré-free moments.

Limitations. Effective as MopNet is, there still remain several extreme cases when it achieves limited success for removing moiré patterns. Figure 12 illustrates challenging scenarios where there exists exceedingly complex and irregular texture such as gravel or pavement surface in the background, and such erratic background will make the edge predictor fail to correctly distinguish the edges of background from moiré gradients, leading to incomplete removal of moiré patterns. However, as shown in Figure 12, our method still provides better restored results compared to the state-of-the-art method [20]. We will improve such cases in our future work.

Acknowledgments. The authors thank Jingyu Yang for providing the results of [23] using our data. This work was supported by the National Natural Science Foundation of China under Grant 61661146005, Grant 61872012 and Grant U1611461.

References

- [1] Bryce E Bayer. Color imaging array, July 20 1976. US Patent 3,971,065. **4**
- [2] Harold C Burger, Christian J Schuler, and Stefan Harmeling. Image denoising: Can plain neural networks compete with BM3D? In *Proceedings of the IEEE Conference on Computer Vision and Pattern Recognition*, pages 2392–2399. IEEE, 2012. **3**
- [3] Jia Deng, Wei Dong, Richard Socher, Li-Jia Li, Kai Li, and Li Fei-Fei. Imagenet: A large-scale hierarchical image database. 2009. **5**
- [4] Jie Hu, Li Shen, and Gang Sun. Squeeze-and-excitation networks. In *Proceedings of the IEEE Conference on Computer Vision and Pattern Recognition*, pages 7132–7141, 2018. **3**
- [5] Gao Huang, Zhuang Liu, Laurens Van Der Maaten, and Kilian Q Weinberger. Densely connected convolutional networks. In *Proceedings of the IEEE Conference on Computer Vision and Pattern Recognition*, pages 4700–4708, 2017. **3**
- [6] Jiwon Kim, Jung Kwon Lee, and Kyoung Mu Lee. Accurate image super-resolution using very deep convolutional networks. In *Proceedings of the IEEE Conference on Computer Vision and Pattern Recognition*, pages 1646–1654, 2016. **6**
- [7] Tae-Hoon Kim and Sang Il Park. Deep context-aware de-screening and rescreening of halftone images. *ACM Transactions on Graphics*, 37(4):48, 2018. **3**
- [8] Diederik P Kingma and Jimmy Ba. Adam: A method for stochastic optimization. *arXiv preprint arXiv:1412.6980*, 2014. **5**
- [9] Christian Ledig, Lucas Theis, Ferenc Huszár, Jose Caballero, Andrew Cunningham, Alejandro Acosta, Andrew Aitken, Alykhan Tejani, Johannes Totz, Zehan Wang, et al. Photo-realistic single image super-resolution using a generative adversarial network. In *Proceedings of the IEEE Conference on Computer Vision and Pattern Recognition*, pages 4681–4690, 2017. **5, 8**
- [10] Stamatis Lefkimmiatis. Universal denoising networks: A novel CNN architecture for image denoising. In *Proceedings of the IEEE International Conference on Computer Vision*, pages 3204–3213, 2018. **3**
- [11] Anat Levin and Yair Weiss. User assisted separation of reflections from a single image using a sparsity prior. *IEEE transactions on Pattern Analysis and Machine Intelligence*, 29(9):1647–1654, 2007. **4**
- [12] Yu Li and Michael S Brown. Exploiting reflection change for automatic reflection removal. In *Proceedings of the IEEE International Conference on Computer Vision*, pages 2432–2439, 2013. **4**
- [13] Bolin Liu, Xiao Shu, and Xiaolin Wu. Demoiréing of camera-captured screen images using deep convolutional neural network. *arXiv preprint, arXiv:1804.03809*, 2018. **3**
- [14] Ding Liu, Bihan Wen, Yuchen Fan, Chen Change Loy, and Thomas S Huang. Non-local recurrent network for image restoration. In *Advances in Neural Information Processing Systems*, pages 1680–1689, 2018. **3**
- [15] Fanglei Liu, Jingyu Yang, and Huanjing Yue. Moiré pattern removal from texture images via low-rank and sparse matrix decomposition. In *IEEE Visual Communications and Image Processing*, pages 1–4, 2015. **1, 2**
- [16] Seungjun Nah, Tae Hyun Kim, and Kyoung Mu Lee. Deep multi-scale convolutional neural network for dynamic scene deblurring. In *Proceedings of the IEEE Conference on Computer Vision and Pattern Recognition*, pages 3883–3891, 2017. **3**
- [17] Kimihiko Nishioka, Naoki Hasegawa, Katsuya Ono, and Yutaka Tatsuno. Endoscope system provided with low-pass filter for moire removal, Feb. 15 2000. US Patent 6,025,873. **1**
- [18] William T Plummer. Anti-aliasing optical system with pyramidal transparent structure, Feb. 5 1991. US Patent 4,989,959. **2**
- [19] Olaf Ronneberger, Philipp Fischer, and Thomas Brox. U-Net: Convolutional networks for biomedical image segmentation. In *International Conference on Medical image computing and computer-assisted intervention*, pages 234–241, 2015. **6**
- [20] Yujing Sun, Yizhou Yu, and Wenping Wang. Moiré photo restoration using multiresolution convolutional neural networks. *IEEE Transactions on Image Processing*, 27(8):4160–4172, 2018. **1, 2, 3, 5, 6, 7, 8**
- [21] Xiaolong Wang, Ross Girshick, Abhinav Gupta, and Kaiming He. Non-local neural networks. In *Proceedings of the IEEE Conference on Computer Vision and Pattern Recognition*, pages 7794–7803, 2018. **4**
- [22] Jingyu Yang, Fanglei Liu, Huanjing Yue, Xiaomei Fu, Chunping Hou, and Feng Wu. Textured image demoiréing via signal decomposition and guided filtering. *IEEE Transactions on Image Processing*, 26(7):3528–3541, 2017. **1, 2**
- [23] Jingyu Yang, Xue Zhang, Changrui Cai, and Kun Li. Demoiréing for screen-shot images with multi-channel layer decomposition. In *IEEE Visual Communications and Image Processing*, pages 1–4. IEEE, 2017. **2, 5, 6, 8**
- [24] Xitong Yang, Zheng Xu, and Jiebo Luo. Towards perceptual image dehazing by physics-based disentanglement and adversarial training. In *AAAI Conference on Artificial Intelligence*, 2018. **3**
- [25] He Zhang and Vishal M Patel. Density-aware single image de-raining using a multi-stream dense network. In *Proceedings of the IEEE Conference on Computer Vision and Pattern Recognition*, pages 695–704, 2018. **3**
- [26] He Zhang, Vishwanath Sindagi, and Vishal M Patel. Image de-raining using a conditional generative adversarial network. *arXiv preprint arXiv:1701.05957*, 2017. **3, 5**
- [27] Kai Zhang, Wangmeng Zuo, Yunjin Chen, Deyu Meng, and Lei Zhang. Beyond a gaussian denoiser: Residual learning of deep cnn for image denoising. *IEEE Transactions on Image Processing*, 26(7):3142–3155, 2017. **6**
- [28] Kai Zhang, Wangmeng Zuo, Shuhang Gu, and Lei Zhang. Learning deep CNN denoiser prior for image restoration. In *Proceedings of the IEEE Conference on Computer Vision and Pattern Recognition*, pages 3929–3938, 2017. **3**